

A Novel Method for Magnetization Transfer Ratio Imaging Without Requiring Separate Saturation Pulse

Jeffrey William Barker^{1,2}, Kyongtae Ty Bae¹, and Sung-Hong Park^{1,3}

¹Radiology, University of Pittsburgh, Pittsburgh, Pennsylvania, United States, ²Bioengineering, University of Pittsburgh, Pittsburgh, Pennsylvania, United States, ³Bio and Brain Engineering, Korean Advanced Institute of Science and Technology, Daejeon, Yuseong-gu, Korea

Purpose: To demonstrate a new method for fast acquisition of magnetization transfer ratio (MTR) imaging utilizing interslice magnetization transfer effects that require no separate saturation pulse.

Introduction: Exchange of magnetization between free water protons and macromolecular protons can lead to magnetization transfer effects (MT). Interslice MT effects that are inherent to multi-slice acquisitions [1] have been used to generate MT contrast for MT asymmetry imaging [2]. In this work, we extend this concept to a new technique for MTR imaging that does not require a separate saturation pulse. We validated the image contrast source by imaging a 4% agar phantom and saline phantom as a control. Finally, we demonstrated the feasibility of *in vivo* MTR imaging by acquiring images in the brain of healthy normal volunteers (N = 5, age 24-49).

Theory: In 2D sequences, slice-selection is achieved by applying a gradient perpendicular to the slice plane, which causes spatially varying spin frequencies. Excitation of a slice of interest is achieved by adjusting RF-pulse frequency. The slice of interest receives on-resonance excitation; however, the rest of the volume receives off-resonance irradiation. Excitation pulses during acquisition of one slice are effectively seen as a train of off-resonance saturation pulses to future slices (Fig. 1). The off-resonance frequency received by neighboring slices is given by $\delta_n = BW \cdot (1 + GAP/THK) \cdot n \cdot \text{sign}(GRAD) \cdot ORD$, in which BW is the bandwidth of the RF-pulse, GAP is the interslice gap; THK is the slice thickness; n is the slice index with positive indices indicating future slices; $\text{sign}(GRAD)$ is the sign of the gradient; ORD is +1 if ascending slice order and -1 if descending slice order. The off-resonance irradiation received by neighboring slices leads to interslice MT effects, which can be exploited as a mechanism for generating contrast by the use of balanced steady state free precession (bSSFP) sequences, which lead to high saturation of the macromolecular pool due to the high flip angle and short repetition time (TR). The interslice gap is set to a high value (e.g. 140% slice thickness) to avoid crosstalk from overlapping slice profiles and so that interleaving two acquisitions gives a full set of images at typical gap size (e.g. 20% slice thickness) [2]. For imaging in the brain, descending slice order should be used to avoid signal contributions from perfusion. Because MT effects accumulate over multiple slices, a few extra “dummy” slices must be collected in the MT-weighted image sets, which can be discarded during reconstruction. Reference images without MT-weighting can be acquired by adding an interslice delay sufficient for T_1 recovery. The MTR value, which measures the percent signal decrease, can be calculated pixel by pixel as $MTR = 100\% \times (S_{MT} - S_{Ref}) / S_{Ref}$, in which S_{MT} and S_{Ref} are the signal intensities of corresponding pixels in the MT-weighted and reference images, respectively.

Methods: All imaging experiments were approved by the Institutional Review Board and performed on a Siemens 3T Trio system (Siemens Medical Solutions, Erlangen, Germany). A 12-element head matrix coil was used for all data acquisitions.

A 4% agar phantom and saline (with 50mM CuSO_4) phantom control were imaged for initial validation of MTR imaging with interslice MT effects. Scan parameters were as follows: TR/TE = 4.56/2.28ms; matrix size = 128x128; field of view = 128x128mm²; slice thickness = 3mm; interslice gap = 3mm; initial dummy PE steps = 10/30 for linear/centric PE order; phase oversampling = 200%; number of averages = 3; RF-pulse BW = 1600Hz; acquisition BW = 501Hz/pixel; number of slices = 9 for MT-weighted images (including dummy slices) and 5 for reference images; interslice delay = 0s for MT-weighted images and 8s for reference images. The off-resonance saturation frequency from the first prior slice was $\delta_{-1} = 3840\text{Hz}$.

For five normal, healthy subjects (age 24-49), MTR images were acquired in the brain. The acquisition parameters were as follows: slice order = descending; slice-select gradient polarity = negative; readout gradient polarity = positive; TR/TE = 4.56/2.28ms; matrix size = 256x256mm²; flip angle = 50°; slice thickness = 3mm; interslice gap = 4.2mm (0.6mm after interleaving); scan direction = axial; PE direction = anterior-posterior; dummy PE steps = 30; phase oversampling = 50%; number of averages = 1; RF-pulse BW = 1600Hz; acquisition BW = 501Hz/pixel; number of slices = 19 and 18 for each interleaved MT-weighted image set (including dummy slices) and 25 for reference images; interslice delay = 0s for MT-weighted images and 6s for reference images; total scan time = 4.3min (1.3min for MT-weighted images and 3min for reference images). The off-resonance saturation frequency from the first prior slice was $\delta_{-1} = 3840\text{Hz}$.

Results and Discussion: Figure 2 shows the results of imaging the 4% agar phantom. The MTR images (top row) show homogeneous MTR values across the slice. Linear PE images showed lower MTR values and visibly lower SNR due to relaxation effects occurring from the start of acquisition to the center line of k-space. The control image, which is expected to have no MT effects, was free from signal contaminations. Together, the agar and control phantom images validate the signal source as MT effects. Figure 3 shows representative high-resolution MTR images using the interslice MTR imaging method. The mean MTR values from regions of interest located in WM of the corpus callosum and frontal GM of the center slice across subjects was $(31.7 \pm 1.0)\%$ and $(21.7 \pm 1.2)\%$, respectively.

The ALADDIN sequence uses a similar acquisition scheme as this work, in which sequential multi-slice bSSFP acquisitions with alternating slice order and slice-select gradient polarity, as well as alternating readout gradient polarity [3] are utilized for interslice perfusion [4] and MT asymmetry imaging [2]. Thus, the addition of reference images to the ALADDIN sequence would allow for the simultaneous acquisition of perfusion, MT asymmetry, and MTR images.

Conclusion: Interslice MTR imaging provides a fast, SAR efficient method for MTR imaging.

References: [1] Dixon, W.T., et al., Magn Reson Imaging, 1990. 8(4): p. 417-22. [2] Park, S.H. and Duong, T.Q., Magn Reson Med, 2011. 65(6): p. 1702-10. [3] Park, S.H., et al., Magn Reson Med, 2012. 68(5): p. 1600-1606. [4] Park, S.H. and Duong, T.Q., Magn Reson Med, 2011. 65(6): p. 1578-91.

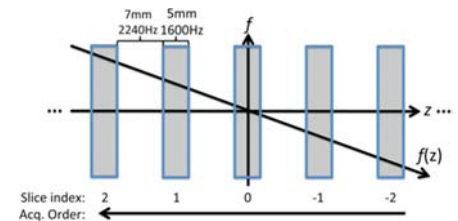


Figure 1. The application of a gradient varies the spin frequencies $f(z)$ linearly in space (z). Excitation of slice 0 will give off-resonance irradiation at frequency offsets of 3840Hz and 7680Hz to slices 1 and 2. Thus, slice 0 received off-resonance irradiation at frequency offsets of 3840Hz and 7680Hz from slices -1 and -2.

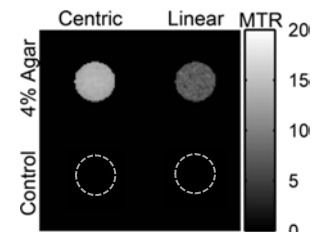


Figure 2. The MTR images of agar show homogenous MTR values. Centric phase encoding showed higher MTR values and visibly better SNR. Control images (saline doped with CuSO_4) were free from MT signals.

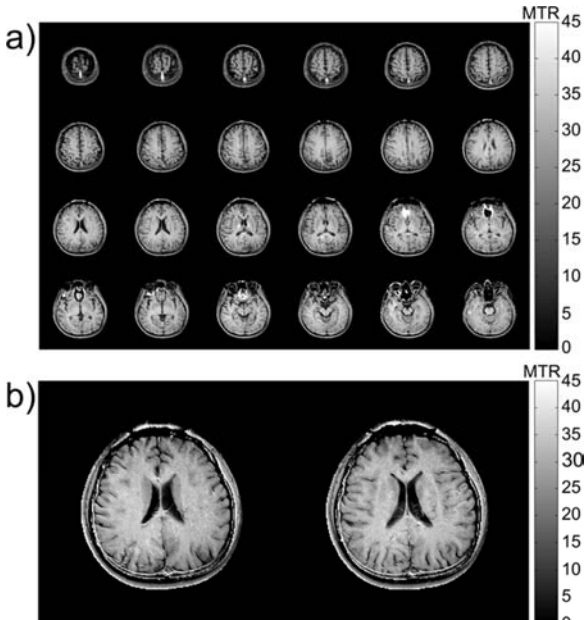


Figure 3. a: High resolution ($1.0 \times 1.0 \times 3.0\text{mm}^3$ with 20% slice gap) MTR images from a representative subject, in which 25 slices (24 of 25 shown) were acquired in ~4min. b: Two slices from the center of the brain enlarged to illustrate the quality of images.